

# Multiple side-band generation for two-frequency components injected into a tapered amplifier

Hua Luo,<sup>1</sup> Kai Li,<sup>1</sup> Dongfang Zhang,<sup>1</sup> Tianyou Gao,<sup>1</sup> and Kaijun Jiang<sup>1,2,\*</sup>

<sup>1</sup>State Key Laboratory of Magnetic Resonance and Atomic and Molecular Physics, Wuhan Institute of Physics and Mathematics, Chinese Academy of Sciences, Wuhan 430071, China

<sup>2</sup>Center for Cold Atom Physics, Chinese Academy of Sciences, Wuhan 430071, China

\*Corresponding author: kjjiang@wipm.ac.cn

Received January 29, 2013; revised February 21, 2013; accepted February 22, 2013;  
posted February 26, 2013 (Doc. ID 184360); published April 1, 2013

We have experimentally studied multiple side-band generation for two-frequency components injected into a tapered amplifier (TA) and demonstrated its effects on atomic laser cooling. A heterodyne frequency-beat measurement and a Fabry–Perot interferometer have been applied to analyze the side-band generation with different experimental parameters, such as frequency difference, injection laser power, and TA current. In laser-cooling potassium40 and potassium41 with hyperfine splitting of 1.3 GHz and 254 MHz, respectively, the side-band generation with a small frequency difference has a significant effect on the number of trapped atoms. © 2013 Optical Society of America  
OCIS codes: 140.3520, 140.4480, 190.4223, 020.3320.

Multiple side bands with an equal frequency spacing have various applications in quantum optics and laser cooling. Zhu *et al.* observed the multiple-mode side-band fluorescence around the resonant transition with a strong dichromatic field coupling two energy levels [1]. Multiple electromagnetic induced transparencies [2] and four-wave mixing have been observed with two coupling components and one probing component in a three-level system [3]. And an arbitrary side band with squeezing has been demonstrated in the experiment [4]. In laser cooling of alkali atoms, two-frequency components are required, one for optical pumping and the other for cooling. The semiconductor laser has become a standard tool in laser cooling due to its easy operation and low cost. But its low output power (generally less than 100 mW) puts a limit on the number of trapped atoms. The output power of a tapered amplifier (TA) can be very high (generally more than 500 mW), which enables us to improve the parameters of trapped atoms. Different spectra have been achieved on the base of a TA. For example, two-frequency components can be simultaneously injected into a TA [5]. A high-power output around 670 nm has been obtained with an external coupling cavity [6,7]. And a TA has been injection seeded with a femtosecond comb [8].

To get a high-power multimode output, multiple frequency components can be simultaneously amplified in a TA to simplify the experimental setup. But at the same time, the wave-mixing process can result in a multiple side-band generation, which may have non-negligible effects on atomic behaviors. Here, we will use a heterodyne frequency-beat measurement with a high resolution (<500 kHz) and a Fabry–Perot interferometer (FPI) to analyze the side-band generation when two-frequency components are injected into a TA. Laser-cooling potassium40 and potassium41 with different hyperfine splitting can demonstrate the effect of side-band generation on the interaction between atoms and light.

Our experimental setup is shown in Fig. 1. Each half-wave plate (from HWP1 to HWP8) is used to rotate the laser polarization direction for adjusting the relative

powers in the two outputs of its following polarization beam splitter (PBS). The output of a diode laser (767 nm wavelength, 30 mW output power, and vertical polarization) is divided into two beams in PBS1. The reflected beam with a vertical polarization is frequency shifted by acousto-optic modulator (AOM1) as a reference beam ( $\nu_r$ ) for the heterodyne frequency-beat measurement. The transmitting beam with a horizontal polarization is again divided into two beams in PBS2, and then one beam is frequency shifted from 40 MHz to 1 GHz using AOM2. The two beams combine together in PBS3 and then are reflected by PBS4. Before being injected into a TA, the beam contains two-frequency components ( $\nu_1$  and  $\nu_2$ ), both of which have a vertical polarization to match the TA polarization. After the TA, the main power is reflected by PBS5 for laser cooling and a small fraction transmits PBS5 for side-band measurement. In PBS6, the reflected beam with vertical polarization is analyzed by an FPI (free spectral range 3 GHz), and the transmitting one overlaps with the reference beam in PBS7 for heterodyne frequency-beat measurement. After PBS8, the two beams with horizontal polarization go through a fiber and are detected by a

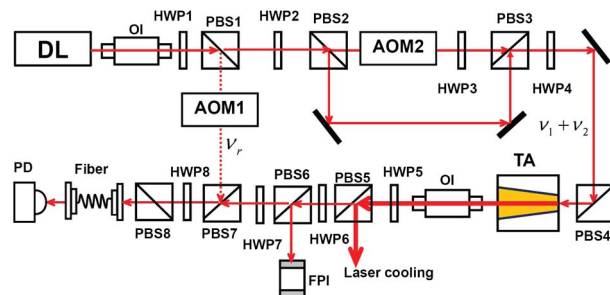


Fig. 1. (Color online) Schematics of the experimental setup. DL, diode laser; OI, optical isolator; HWP, half-wave plate; PBS, polarization beam splitter; AOM, acousto-optic modulator; TA, tapered amplifier; PD, high-speed photodetector; FPI, Fabry–Perot interferometer. The dotted line indicates the reference laser beam.

high-speed photodetector (Newport, Model 1343, 25 GHz bandwidth). For our used TA (UniQuanta Tech, Model TAL100, spectrum range 750–775 nm), the output power is 700 mW in 21°C when the injection power is 14 mW and the TA current is 1.8 A. The apertures of the front and rear facets are 3 and 190  $\mu\text{m}$ , respectively, and both facets are antireflection coated with 0.01%. The chip is based on the semiconductor material GaAs and the amplification length is 2.5 mm. For our frequency-beat measurement, the two beams coming from one diode laser can produce a stable wave mixing due to a good phase coherence.

In our experiment, we use a heterodyne measurement to analyze side-band generation because of the following three reasons: (1) an FPI cannot distinguish different components for a small frequency difference due to its limited resolution. For our applied FPI, the resolution is about 100 MHz. (2) The frequency beat between the high-order side bands is too small to be detected due to its low-power distribution. (3) In the homodyne measurement, different pairs of components may contribute to the same frequency-beat peak. Meanwhile, in the heterodyne measurement, different frequency components can be distinguished clearly. In Fig. 2(a), the powers of the reference beam and the main beam are 0.67 and 2.28 mW, respectively. The frequency difference between the two injection components is 80 MHz,  $\delta = \nu_2 - \nu_1 = 80$  MHz, and the reference component is between these two components,  $\Delta = \nu_2 - \nu_r = 20$  MHz and  $\nu_r - \nu_1 = 60$  MHz. For positive side bands,  $f_{+n} = \Delta + n\delta$ , and for negative side bands,  $f_{-n} = (\delta - \Delta) + n\delta$ , where  $n$  is the order of the side bands. When  $n = 0$ , the signals correspond to the two injection frequencies ( $\nu_2$  and  $\nu_1$ ). All the frequency components (including injection components and side bands) are indicated in Fig. 2(a). Here, we can observe the sixth-order side-band generation, which is the highest order that has been experimentally obtained in a TA. There are also homodyne frequency-beat signals between different components in the output of the TA,  $f_m = m\delta$ , where

$m = 1, 2, 3, \dots, p - 1$  and  $p$  is the total number of the frequency components. Only up to  $m = 7$  signal can be distinguished in our detection sensitivity, and the frequency beat between higher-order side bands is negligibly small. We also perform the heterodyne frequency beat for a 200 MHz difference, where  $\nu_2 - \nu_1 = 200$  MHz and  $\nu_2 - \nu_r = 60$  MHz. The frequency-beat signals are indicated in the inset of Fig. 2(a), and only three side bands (not including the sign of the order) can be detected. When an FPI is applied to perform the measurement, the side-band number is also three, as shown in Fig. 3(a). For frequency differences of 280 and 360 MHz, the measured numbers of the side band with these two methods are also the same. As shown in Fig. 2(b), the side-band number decreases as the frequency difference increases.

Multiple side bands originate from wave mixing when different frequency components overlap in a TA. This nonlinear process results in the laser power distributing among different side bands. An FPI is applied to measure the power distribution among different side bands for a 200 MHz frequency difference. As shown in Fig. 3(a), there exist positive and negative third-order side bands. When the injection powers of the two components are equivalent, side bands distribute almost symmetrically on both sides. Throughout this Letter the side-band power is denoted by its percentage ratio in the total output for simplification. Since the signal for the third-order side band will be indistinguishable in a small TA current, we only include the experimental results for positive and negative two orders. As shown in Fig. 3(b), the power of each side band almost remains unchanged with different TA current. This implies that the two components undergo wave mixing first to get multiple side bands and then are amplified proportionally. The small power difference of the same order side band (for example,  $+\delta$  and  $-\delta$ ) mainly comes from the power imbalance between injection components.

Figure 4 shows that the total power in all side bands almost remains unchanged at 23% with the TA current varying as indicated in Fig. 3(b). It is also shown in Fig. 4 that the total power increases from 14% to 27% when the

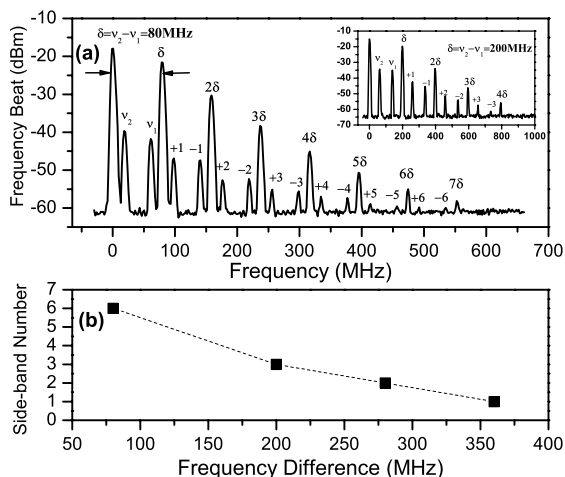


Fig. 2. Generated side bands versus the frequency difference, where the injected power of both components is 15 mW and the TA current is 1.8 A. (a) Frequency-beat signal for an 80 MHz frequency difference (the inset is for a 200 MHz frequency difference). (b) Side-band number versus the frequency difference.

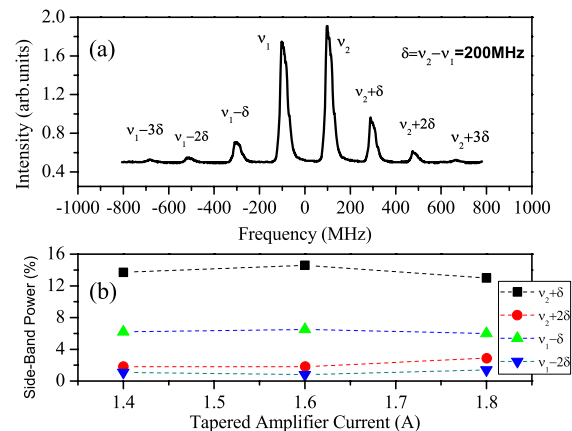


Fig. 3. (Color online) Power distribution of each side band with a 15 mW injection laser power and a 200 MHz frequency difference. (a) Side-band signal measured with an FPI. In a 1.8 A TA current, up to  $+3\delta$  and  $-3\delta$  side bands are obvious on the spectrum. (b) Power distribution of each side band. The black square is for  $+\delta$ , the green uptriangle for  $-\delta$ , the red circle for  $+2\delta$ , and the blue downtriangle for  $-2\delta$ .

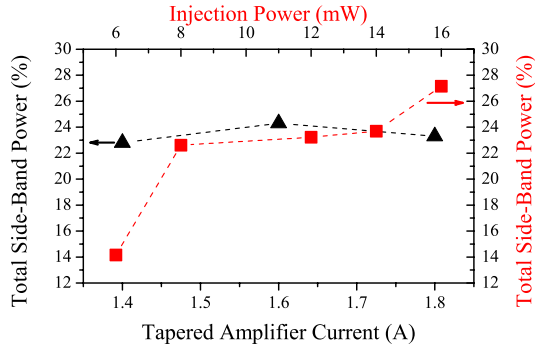


Fig. 4. (Color online) Total power of all side bands. The black triangle denotes the total power versus the TA current, and the red square denotes that versus the injection power.

injection laser power increases. The multiple side-band generation results from a nonlinear process in the solid material, and it should be enhanced in the saturation regime. So, the wave-mixing process will become more dominant with a higher injection power.

Multiple side-band generation should have effects on the interaction between atoms and light. For example, in atomic laser cooling, side-band generation would decrease the power of the cooling light and additional excitations would destroy trapped atoms. To verify this prediction, we first perform laser cooling of potassium40 with a 1.3 GHz hyperfine splitting in the ground state. Two equivalent frequency components with a 1.3 GHz difference are injected into a TA and only 35 mW of output power is used to cool the atoms. The number of trapped atoms is  $4.2(1.3) \times 10^8$ . As a comparison, we directly use two equivalent laser beams with a 1.3 GHz frequency difference and a total 35 mW laser power to perform the experiment. The trapped atom number is  $3.7(1.5) \times 10^8$  in this condition. The similar numbers of obtained atoms demonstrate no obvious effect of the side band. But for potassium41 with only a 254 MHz hyperfine splitting, the trapped atom number is  $1.8(0.8) \times 10^8$  with a two-frequency injection and  $2.1(1.0) \times 10^9$  without the two-component injection. The one order of magnitude difference on the trapped atomic numbers shows a significant effect of the side-band generation. From our measurement, the total side-band power is about 20% for a 254 MHz frequency difference and below our detection

sensitivity for a 1.3 GHz difference. This study demonstrates that the two-frequency injection in a TA can afford a convenient way to simplify the experimental setup on one side. But on the other side, multiple side-band generation has a notable effect on the atomic behaviors if the frequency difference is small. Laser-cooling potassium40 is our starting point to realize degenerate Fermi gases.

In this Letter, heterodyne frequency-beat measurement is for the first time, to the best of our knowledge, applied to analyze side-band generation in a TA. This method is still efficient for a small frequency difference due to its high spectrum resolution. Also, an FPI is applied to explore the side-band generation with different parameters, such as frequency difference, TA current, and injection laser power. Injection of two-frequency components into a TA has been widely employed in laser cooling (for example, [9]), and this indicates the significance of a TA with a multiple-frequency injection. But the authors of previous works did not consider the effect of side-band generation. In this Letter, laser-cooling potassium40 and potassium41 demonstrate its obvious effect on the interaction between atoms and light.

This work is supported by the NSFC (Grant No. 11004224) and NFRF-China (Grant No. 2011CB921601).

## References

1. Y. F. Zhu, Q. L. Wu, A. Lezama, D. J. Gauthier, and T. W. Mossberg, *Phys. Rev. A* **41**, 6574 (1990).
2. J. Wang, Y. F. Zhu, K. J. Jiang, and M. S. Zhan, *Phys. Rev. A* **68**, 063810 (2003).
3. G. Q. Yang, P. Xu, J. Wang, Y. F. Zhu, and M. S. Zhan, *Phys. Rev. A* **82**, 045804 (2010).
4. M. Arikawa, K. Honda, D. Akamatsu, S. Nagatsuka, K. Akiba, A. Furusawa, and M. Kozuma, *Phys. Rev. A* **81**, 021605(R) (2010).
5. G. Ferrari, M. Mewes, F. Schreck, and C. Salomon, *Opt. Lett.* **24**, 151 (1999).
6. T. Q. Tien, M. Maiwald, B. Sumpf, G. Erbert, and G. Tränkle, *Opt. Lett.* **33**, 2692 (2008).
7. M. Chi, G. Erbert, B. Sumpf, and P. M. Petersen, *Opt. Lett.* **35**, 1545 (2010).
8. F. C. Cruz, M. C. Stowe, and J. Ye, *Opt. Lett.* **31**, 1337 (2006).
9. G. Modugno, G. Ferrari, G. Roati, R. J. Brecha, A. Simoni, and M. Inguscio, *Science* **294**, 1320 (2001).